Nitrogen to phosphorus ratio shapes bacterial community involved in cellulose decomposition and copper contamination alters their stoichiometric demand

Ziming Wang, Aurélie Cébron, Vincent Baillard, Michael Danger

Nitrogen to phosphorus ratio shapes bacterial community involved in cellulose decomposition and copper contamination alters their stoichiometric demand

Ziming Wang[1*], Aurélie Cébron[2], Vincent Baillard[1], Michael Danger[1,3]

[1] Université de Lorraine, CNRS, LIEC, F-57000, Metz, France

[2] Université de Lorraine, CNRS, LIEC, F-54000, Nancy, France

[3] Institut Universitaire de France (IUF), F-75000, Paris, France

[*]Corresponding author. Université de Lorraine, CNRS UMR 7360, Laboratoire Interdisciplinaires des Environnements Continentaux (LIEC), 8 Rue Général Delestraint, 57070 Metz, France. Tel: +33 3 72 74 89 38. E-mail: ziming.wang@univ-lorraine.fr

Abstract

All living organisms have theoretically an optimal stoichiometric nitrogen:phosphorus (N:P) ratio below and beyond which their growth is affected but data remain scarce for microbial decomposers. Here, we evaluated optimal N:P ratios of microbial communities involved in cellulose decomposition and assessed their stability when exposed to copper Cu(II). We hypothesized that (1) cellulose decomposition is maximized for an optimal N:P ratio, (2) copper exposure reduces cellulose decomposition and (3) increases microbial optimal N:P ratio, (4) N:P ratio and copper modify the structure of microbial decomposer communities. We measured cellulose disc decomposition by a natural inoculum in microcosms exposed to a gradient of N:P ratios at three copper concentrations (0, 1 and 15 µM). Bacteria were most probably the main decomposers. Without copper, cellulose decomposition was maximized at an N:P molar ratio of 4.7. Contrary to expectations, at high copper concentration, the optimal N:P ratio (2.8) and the range of N:P ratios allowing decomposition were significantly reduced and accompanied by a reduction of bacterial diversity. Copper contamination led to the development of tolerant taxa probably less efficient in decomposing cellulose. Our results shed new lights on the understanding of multiple stressor effects on microbial decomposition in an increasingly stoichiometrically imbalanced world.

Key words:

N:P ratio, metal contamination, ecological stoichiometry, nutrient immobilization, nutrient mineralization, bacterial diversity, microbial decomposer

1. Introduction

Decomposition is the biological process that leads to mass reduction and transformation of dead organic matter (Gessner *et al.* 2010). It is a ubiquitous process and a fundamental link in the biogeochemical cycles of elements and central for ecosystem functioning. Plant litter decomposition is a complex process controlled simultaneously by intrinsic factors, environmental factors and abundance and diversity of biological actors (Gessner *et al.* 2010; Bani *et al.* 2018). Some heterotrophic microorganisms, including both fungi and bacteria, form the functional group of microbial decomposers which are the main actors of decomposition (Gessner, Chauvet and Dobson 1999). Among the environmental factors likely to impact the plant litter decomposition process, nutrient availability in the surrounding environment of the litter plays a crucial role (Güsewell and Verhoeven 2006; Güsewell and Gessner 2009; Woodward *et al.* 2012). Plant litter is generally nutrient depleted (Moore *et al.* 2004), and microbial decomposers must balance their nutrient requirements through the consumption of mineral elements coming from their environment (a process called nutrient immobilization: Harte and Kinzig 1993; Daufresne and Loreau 2001). When these requirements are satisfied, these organisms are able to efficiently decompose plant litter, converting it into their biomass. At the same time, they also release inorganic carbon through their respiration and nutrients through their exoenzymatic activities, these elements being considered as recycled back into ecosystems (inorganic carbon and nutrient releases correspond to the mineralization process: Harte and Kinzig 1993). Several reviews clearly confirmed the stimulating effects of nutrient enrichment on decomposition rates (Ge *et al.* 2013; Ferreira *et al.* 2015b; Zhang *et al.* 2018), suggesting the idea that a balanced nutrient availability which allows the microorganisms to optimally fulfil their nutrient demand should be beneficial for maximizing their decomposition activity. A precise knowledge of the elemental requirement of microbial decomposers is thus an essential prerequisite for

53 predicting the speed and intensity of litter decomposition as well as nutrient and carbon
54 releases.

55 In the ecological stoichiometry framework, the imbalance between consumer
56 requirements and elements availability is often referred to as “stoichiometric constraints”
57 (Sterner and Elser 2002). Among all the necessary chemical elements that ensure living
58 organism growth, nitrogen (N) and phosphorus (P) are generally the most commonly
59 considered. N is one of the main components of amino acids (proteins), and P is, among
60 others, a fundamental component of nucleic acids (DNA and RNA). Litter decomposition is
61 frequently controlled by N and P availability in the medium (Woodward *et al.* 2012). For
62 microbial decomposers, the overall litter and environmental N:P ratio may therefore be a
63 potential indicator for determining whether the N or P might be limiting for microorganisms
64 growth and activity, at least during the early stage of decomposition when carbon availability
65 is not limiting (Tessier and Raynal 2003).

66 While the specific optimal elemental ratios have long been studied in plants (e.g. Tilman
67 1985) and animals (e.g. Frost *et al.* 2006), data are far less available for microorganisms.
68 Using natural microbial inoculum, Güsewell and Gessner (2009) shown that cellulose and
69 plant litter decomposition were maximized at intermediate available N:P ratios, these ratios
70 corresponding to optimal N:P ratios for the decomposition process at the community level.
71 Changes in the available N:P ratios also resulted in altered balance between microbial
72 decomposers, as shown by changes in the bacteria to fungi ratio along their N:P gradient.
73 From a stoichiometric viewpoint, such changes in community structure could result from
74 competitive exclusion and the selection of species based on their optimal nutrient
75 requirements along the N:P availability gradient (Danger *et al.* 2008). Thus, based on
76 microbial nutrient requirements, the relative N to P availability should, at least partly,
77 determine community structure and composition. Concerning the decomposition process,

these species replacements are expected to maximize nutrient uptake and reduce variations in litter decomposition efficiency (Fanin *et al.* 2013).

Giving the importance of microbial optimal nutrient ratios for the decomposition process and community structures, understanding the response of these optimal ratios to environmental stressors might be of particular interest. If multiple environmental stressors impact microbial diversity, plant litter decomposition may be affected (Niyogi *et al.* 2009; Gessner *et al.* 2010; Ferreira *et al.* 2015a; Tolkkinen *et al.* 2015). Both nutrient availability (Falkowski *et al.* 2000) and ratios (Elser *et al.* 2009; Peñuelas *et al.* 2013) can be problematic for ecosystem functioning due to changes in nutrient balance. Metal contamination is another major recurrent stressor. Metals have long been shown to reduce plant litter decomposition rates in lands (Berg *et al.* 1991) and in streams (Duarte *et al.* 2008). The number of litter-colonizing fungus decreases in presence of high metal concentrations (Solé *et al.* 2008). Microbial activity is lower in metal polluted environments (Niyogi *et al.* 2009). Copper (Cu) represents a classical model of metallic contaminant. This metal is still actively used in agriculture, resulting in its accumulation in soils and leaching into surface water ecosystems. Cu has been largely studied and is known to alter microbial community structures (Wakelin *et al.* 2010; Keiblinger *et al.* 2018) and affect litter decomposition (Fernández *et al.* 2015).

In this study, using Cu as a model of contaminant, we investigated its impact on the optimal elemental N:P ratios for cellulose decomposition by microbial decomposers. We hypothesized that (H1) cellulose decomposition rate reaches its maximum at an optimal N:P ratio; (H2) high Cu concentration reduces the overall cellulose decomposition rate; (H3) due to increased N-demand for detoxification and reduced microbial growth, the optimal N:P ratio increases under higher Cu contamination, and (H4) both N:P ratio and the presence of Cu interactively affect the composition of microbial decomposer communities. Since natural plant litter nutrient content is often variable (Cornwell *et al.* 2008), pure cellulose,

representing a part of plant cell walls, was used as a model carbon substrate to control N and P quantities, as successfully used in the past (Hopkins *et al.* 1990; Chew, Obbard and Stanforth 2001; Güsewell and Gessner 2009). To test our hypotheses, we quantified the decomposition of cellulose discs by a natural inoculum of microbial decomposers in microcosms under laboratory-controlled conditions. Decomposition was followed along a gradient of available N:P ratios in liquid culture media and under three concentrations of dissolved Cu: 0 µM, 1 µM and 15 µM. After 79 days of incubation, we measured the mass loss of the cellulose discs, the quantities of N and P immobilized on the discs by microbial decomposers and we analysed the abundance and diversity of the microbial decomposers.

2. Material and methods

2.1. Microbial inoculum preparation

Leaves (mainly beech) were collected in 2015, by using suspended filets around trees (1 m above ground) in the forest near the Maix stream in the Vosges Mountains (N53.9143° E27.5791°). In early 2018, eight litterbags (500 µm mesh size) each containing 5 g of leaves (dry weight) were submerged in the same stream to allow bacterial and fungal colonization. The bags were retrieved after 14 days along with samples of stream water. Leaf litter contained in the bags were gathered. Microbial inoculum was prepared by putting 20 g (fresh weight) of leaf litter in 5 L Erlenmeyer flasks with 1 L of fresh stream water, incubated under gentle agitation and aerobic condition for 48 hours at 18 °C. After the incubation, water was separated from large litter debris by passing through a sieve (1 mm mesh size) and was left at 4 °C to decant for 2–3 hours before collecting the supernatant. This microbial inoculum was stored for less than 24 hours at 4°C prior its use for the experiment.

The initial number of fungal spores and bacteria was determined on aliquots of the inoculum. Fungal spores were counted under an optical microscope, inoculum was fixed with formaldehyde (2%) and stained with Trypan blue (0.05%) before being filtered (Millipore

MF™ 5.0 µm SMWP02500). Bacteria were counted through DAPI (1 µg mL^{-1}) staining after filtration (Whatman Nucleopore Track-Etch membrane 25 mm, 0.2 µm). Seven images were taken using an epifluorescence microscope (Nikon C-HGFIE equipped with a DS-Qi1Hc CCD camera) and were analysed using a NIS-Elements BR software (Nikon). Although we planned to have a mixed inoculum, the microcosms were largely inoculated with bacteria (c.a. 9.6×10^7 bacteria per microcosm) and no fungal spores but with a few mycelia fragments (see discussion).

2.2. Microcosm preparation

The microcosms were prepared under sterile condition, following the model from a previous study (Güsewell and Gessner 2009). In a plastic Petri dish (Ø 90 mm) containing 50 g of river sand and covered by a nylon mesh (250 µm porosity), five cellulose discs of Ø 22 mm were placed (Fig.S1). The river sand was sieved (< 2 mm), washed, dried and burned at 450 °C for over four hours to sterilize and remove all traces of organic material. The cellulose discs were cut out from cellulose paper filter (Whatman ashless 110 mm, GE), sterilized and were used as the only carbon source for microorganisms. The total cellulose dry mass introduced into each microcosm was 181.5 ± 5.7 mg (36.3 ± 1.2 mg per disc).

Each microcosm was filled with 18.5 mL of a sterilized COMBO mineral medium containing 36.8 mg L^{-1} $CaCl_2 \cdot 2H_2O$, 37.0 mg L^{-1} $MgSO_4 \cdot 7H_2O$, 12.6 mg L^{-1} $NaHCO_3$, 28.4 mg L^{-1} $Na_2SiO_3 \cdot 9H_2O$ and 24.0 mg L^{-1} H_3BO_3 (Kilham *et al.* 1998) Nitrogen (N), phosphorous (P) and copper (Cu) were also included but with different concentrations to obtain desired N:P ratios and Cu contamination levels.

Seven N:P ratios (molar) were created by varying the amount of both N and P in each medium using NH_4NO_3 for N, and a mixture of KH_2PO_4 and K_2HPO_4 (3.85/6.15 v/v, for pH 7) for P. The seven N:P ratios were 1.2, 3.7, 11, 33, 100, 300 and 898 with a global supply level of 0.75 [geometric mean of N and P mass in mg for all N:P ratios, i.e. in a microcosm,

153 $(m_N \times m_P)^{0.5} = 0.75$, see Güsewell and Gessner 2009]. Three Cu contamination levels (0, 1
154 and 15 µM) were tested by adding $CuSO_4 \cdot 5H_2O$ to each medium. The initial concentrations
155 of N, P and Cu were verified. N and P reached at least 86.4 % of their nominal values, which
156 made the practical N:P ratios vary between 93.9 % and 97.5 % of the theoretical values.
157 Measured copper concentrations were 0.69 ± 0.06 µM and 13.33 ± 0.83 µM for the media
158 containing 1 and 15 µM respectively.

159 A total of 21 conditions (seven N:P ratios × three [Cu]) were tested. Each condition was
160 replicated in five microcosms. Additionally, controls without inoculum were included.

161 The inoculation was done by dispensing 300 µl of freshly prepared and well-homogenized
162 inoculum directly onto each cellulose disc (1.5 mL per microcosm). The microcosms were
163 then placed in dark boxes and kept in an incubator at 18 °C. A water tray was placed in each
164 box to maintain humidity and avoid media evaporation. Humidity of each microcosm was
165 monitored every two weeks during the incubation period. If necessary, water levels were
166 adjusted with MilliQ ultrapure sterile water. Since we were interested in early stages of
167 cellulose decomposition, we initially planned to stop the experiment when ca. 35-50% of
168 detritus mass loss was reached. At day 79, some of the cellulose discs were becoming almost
169 transparent suggesting an advanced stage of decomposition, thus we decided to stop the
170 experiment. Each cellulose disc was collected and conserved individually. To take into
171 account potential heterogeneity between discs in each microcosm, the purpose of each disc
172 was decided randomly. Two discs were freeze-dried and used for cellulose mass loss
173 calculation, one of them was then used for total N and P quantification and the other one was
174 kept for ergosterol extraction. A third disc was used for DNA extraction, and the last two
175 discs were stored at -20 °C as backup.

176 *2.3. Mass loss, ergosterol and N P content*

177 Cellulose mass loss was determined by weighting the two freeze-dried discs to the nearest
178 0.1 mg. Subsequently, one of the discs was used to analyse total N and P content (70 samples,
179 seven N:P ratios × four replicates for [Cu] 0 µM, and seven N:P ratios × three replicates for
180 [Cu] 1 µM and 15 µM). Those discs were reduced into fine powder using Ø 3 mm, clean,
181 steel grinding balls and a bead beater (Mixer Mill, Retsch MM301). Between 1.5 and 2.0 mg
182 of powder was put into tin capsules (Säntis Analytical SA7698110) and used to analyse the
183 total N quantity by an elementary analyser (Carlo Erba NA 2100). The total P quantity was
184 analysed by first digesting 2.0 to 2.5 mg of the powder in 10 mL of NaOH (0.1 M) and
185 $Na_2S_2O_8$ (0.125 M) for two hours at 10^5 Pa (1 bar) 120 °C. After cooling, P was measured on
186 the digested solutions using molybdate blue colorimetric method at 880 nm (ISO 6878:2004).
187 The second freeze-dried disc was used to determine ergosterol content (estimation of fungal
188 biomass). During inoculum preparation and incubation, absence of fungal spores and
189 development has been noted, Real-Time qPCR of fungal 18S rRNA genes also resulted low
190 copy numbers (see below). To confirm this result, only one replicate per condition (21
191 samples) was extracted and analysed for ergosterol, confirming the extremely low abundance
192 of active fungi. Ergosterol extraction and HPLC analyse followed a standard protocol
193 (Gessner 2005). Briefly, the cellulose disc was placed into a KOH/methanol (8 g L^{-1}) solution
194 overnight at 4 °C, then heated at 80 °C during 30 min for extraction. The extracts were loaded
195 into SPE cartridges (Oasis HLB 30 µm Extraction Cartridge). Ergosterol was eluted in 1.4 mL
196 isopropanol and stored at -20 °C until HPLC analyses. Extractions were carried out in a series
197 of 12 with 11 samples and a positive control with known concentration of HPLC grade
198 ergosterol (>95 %, Sigma Life Science). HPLC analyses were assured by Chromaster Hitachi
199 (Pump 5110, Autosampler 5210, UV Detector 5410), using LiChrospher RP18 column

(LiChroCART 250-4 HPLC cartridge, Merck), equipped with a column thermostat set at 33 °C (Jetstream 2 plus).

2.4. Molecular analyses (DNA extraction, qPCR, NG-sequencing, OTU analyses)

Total genomic DNA was extracted from one disc of each microcosm (65 samples, seven N:P ratios × three [Cu] × three replicates plus two replicates of the initial inoculum), using the PowerSoil DNA Isolation Kit (MO BIO), and following the manufacturer protocol. Between 3 and 7 ng μL^{-1} of total DNA (measured with a Shimatzu spectrophotometer equipped with a Traycell tank) were recovered from each cellulose disc.

Real-Time qPCR targeting the 16S and 18S rRNA genes (bacteria and fungi, respectively) were performed as described in Cébron *et al.* (2008) and Thion *et al.* (2012). The number of 16S and 18S rRNA gene copies was used to estimate bacterial and fungal relative abundances. The primer pairs used were 968F (5'-GAACGCGAAGAACCTTAC-3') and 1401R (5'-CGGTGTGTACAAGACCC-3') for bacterial 16S rDNA (Nübel *et al.* 1996) and Fung5F (5'-GTAAAAGTCCTGGTTCCCC-3') and FF390R (5'-CGATAACGAACGAGACCT-3') for fungal 18S rDNA (Smit *et al.* 1999; Vainio and Hantula 2000). The amplification mix was prepared in 20 µL with: 10 µL 2× iQ SyberGreen Supermix (Bio-Rad); 0.8 µL of each primer (10 µM); 0.4 µL of 3% bovine serum albumin (BSA); 0.2 µL of dimethyl sulfoxide (DMSO); 0.08 µL of T4 bacteriophage gene-32 product (QBiogene); 6.72 µL of DNA-free distilled water and 1 µL of template DNA or distilled water (negative control) or ten-time dilutions of standard plasmids from 10^8 to 10^1 copies μL^{-1}). The amplification programmes used for Real-Time qPCR were as follows: 95 °C for 5 min, 40 cycles with 20 s at 95 °C, 20 s at the primers specific annealing temperature (56 °C and 50 °C for 16S and 18S rDNA, respectively), 30 s at 72 °C and 5 s measurement of SYBR® Green I signal at 82 °C or 80 °C (for 16S and 18S rDNA, respectively), followed by a melting curve analysis from 50 °C to 95 °C.

For bacterial 16S rRNA gene amplicon-sequencing, the primer pair used for the first-step PCR were 341F (5'-CCTACGGGAGGCAGCAG-3'; Muyzer, de Waal and Uitterlinden 1993) and 787R (5'-GGACTACNVGGGTWTCTAAT-3'; Caporaso *et al.* 2011), each attached to an adaptor for a second PCR. The amplification mix was prepared for 50 µL final volume with: 10 µL 5× HF Buffer; 1 µL of dNTP (10 mM); 0.25 µL of dimethyl sulfoxide (DMSO); 0.1 µL of T4 bacteriophage gene32 product (QBiogene); 1.5 µL of $MgCl_2$ (50 mM); 1 µL of each primer (10 µM); 33.05 µL of DNA free distilled water; 0.1 µL of Phusion polymerase (Thermo Scientific) and 2 µL of DNA samples (or distilled water for negative control). 30 cycles of amplification at 56°C annealing temperature were performed. These first-step PCR products containing unpurified DNA were then sent to Microsynth (Next Generation Sequencing Department, Microsynth AG, Switzerland) for the second-step PCR and MiSeq 2×250 bp paired-end sequencing (Illumina).

A total of 4 443 671 paired-end reads from the 65 samples (accessible on SRA-NCBI database under BioProject accession number PRJNA820766) were obtained. Paired-end sequences were processed for quality filtering and clustered into operational taxonomic unit (OTU) at 97% using Mothur (v1.44.3; Schloss *et al.* 2009) and following MiSeqSOP (first access date: 14 December 2020; (Kozich *et al.* 2013)). Taxonomy was assigned using SILVA ssu132 database. Singletons and sequences not affiliated to bacteria were removed. The final dataset comprised 1 896 248 sequences ranging from 4576 to 81 348 sequences per sample. Finally, the dataset was rarefied to the lowest number of sequences *per* sample (i.e. 4576 reads/sample, see Fig.S2 for rarefication curves) to compare the diversity of 2219 OTUs (including data from the initial inoculum). By doing so, we had sufficient sequencing depth and statistical power to compare between conditions although some OTUs had been excluded. Alpha diversity was expressed by calculating Chao1 richness and Shannon diversity indices (Hill *et al.* 2003) using Mothur.

2.5. Statistical Analyses

All modelling and statistical analyses of our results were carried out with R software (v4.1.0; R Core Team 2022). The N:P ratios were log transformed prior to all analyses.

We assume the cellulose mass loss caused by microbial decomposers follows a biphasic tendency (symmetric "bell-shape" curve) alongside the log transformed gradient of N:P ratios. For this reason, the cellulose disc mass loss data was fitted using a Gaussian type model with four parameters:

$$y = (h - d)\, exp\left(-2\left(\frac{x - e}{w - e}\right)^2\right) + d$$

Where y is the cellulose disc mass loss in percentages, x is the log-transformed value of N:P ratio, h is the maximum y value which is the height of the curve peak (i.e. the maximal mass loss), d is the mass loss for very low and very high N:P ratios (i.e. the minimal mass loss which is considered to be constant regardless of the N:P ratio), w (>0) is a shape parameter which controls the width of the "bell", it is the N:P ratio below which the mass loss reaches 97.5 % of d. It can also be seen as the highest N:P ratio beyond which the additional mass loss over d is negligible. Finally, e (>0) is the value of x which corresponds to the maximum y value, it is the log of the N:P ratios where the maximal mass loss can be observed. (Fig.1a adapted from Larras *et al.* 2018)

Two-way analysis of variance (ANOVA) was used to evaluate the effect of N:P ratio, [Cu] and their interaction on cellulose mass loss, and immobilized N and P quantities. In case of a *p*-value lower than 0.05, Tukey HSD *Post-Hoc* tests were performed to determine which treatments differ significantly from others. When ANOVA was inapplicable, nonparametric Kruskal-Wallis test followed by Wilcoxon-Mann Whitney *Post-Hoc* test was applied. Levene's test was applied to verify homogeneity of variance between conditions. The linear correlations between cellulose mass loss and OTU numbers, Chao1 or Shannon indices of all

three Cu contamination levels were obtained by calculating the Pearson's correlation coefficient. Levene's test was from "car" R package (v3.0-13; Fox and Weisberg 2019), other tests were from the "stats" package (v4.2.0; R Core Team 2022).

The beta diversity based on Bray-Curtis dissimilarity was represented using non-metric multidimensional scaling (NMDS) analysis with two dimensions using the "metaMDS" function of the "vegan" R package (v2.5-7; Oksanen *et al.* 2020). The differences in community composition between each level of [Cu] were tested by permutational multivariate analysis of variance (PerMANOVA) with 999 permutations using the "adonis2" function.

In an attempt to identify bacterial taxa that stand out the most under contrasted treatments, indicator species were analysed. The indicator values (IndVal, <1) of OTUs were calculated using the "multipatt" function of the "indicspecies" package (v1.7.9; de Cáceres, Legendre and Moretti 2010). We used the group-equalized IndVal (IndVal.g) index to find OTUs that were proportionally more likely to be present at a group. By limiting the index between 0.7 and 1 as done previously by other studies (Demircan *et al.* 2018), we can focus on the most relevant OTUs. The higher the value, the more likely an OTU was abundant in that group. Based on result similarities of bacterial diversities and cellulose decomposition at different N:P ratios and [Cu] (see results section), we have decided to merge these results into four groups: 0 and 1 µM of [Cu] were grouped together as "low Cu (CL)" and the group of 15 µM as "high Cu (CH)", we omitted all the samples of N:P ratio of 33 as it is an intermediate ratio and then grouped the three lower ratios together and the three higher ratios together (as "RL" and "RH", respectively), thus forming four groups: CLRL, CLRH, CHRL and CHRH. The indicator species analysis was performed with 9999 permutations on the rarefied dataset of 1603 OTUs (excluding data from the initial inoculum).

3. Results

3.1. Cellulose disc mass loss – Optimal N:P ratio

Cellulose discs lost up to 30 % of their initial dry mass. Mass losses depended on [Cu] (ANOVA, F = 62.365, Pr < 0.001) and supplied N:P ratio (F = 108.317, Pr < 0.001), with a significant interaction (F = 3.652, Pr < 0.001). Fig.1b shows the mean values of empirical mass losses (points) and the statistical models (curves). For all three Cu contamination levels, the maximal mass loss occurred at the supply ratio of 3.7 and the minimal mass loss occurred at ratios greater than 100. For lower [Cu] (0 and 1 µM of Cu), the minimum mass loss was about 10 % while it was as low as about 2 % for the group of 15 µM.

Values of each parameter and their confidence intervals (CI, 95 %) were extracted from models. Optimal N:P ratios (parameter *e*, Fig.1c) decreased with increasing [Cu]. The CI showed that the optimal N:P ratios for 0 and 15 µM of Cu (4.7 and 2.8, respectively) differed significantly from each other. Minimal mass losses (parameter *d*, Fig.1d) showed no difference between 0 and 1 µM of Cu (8.0 % and 8.3 %, respectively) but both were significantly different from that of 15 µM (1.5 %). On the other hand, the maximal mass losses (parameter *h*, Fig.1e) between all three groups were not significantly different from each other (28.6 %, 25.3 % and 23.9 % for 0, 1 µM and 15 µM of Cu, respectively), the value tended to decrease with increasing [Cu]. Although the maximal effective N:P ratio (parameter *w*, Fig.1f, N:P ratio beyond which the mass loss is minimal and stays constant) values were not significantly different among the three Cu contamination levels, they were reduced from 102.4 to 33.6 between 0 µM to 15 µM of Cu.

3.2. Immobilized N and P quantities on cellulose discs

The quantity of immobilized N was independent of [Cu] (ANOVA, F = 1.301, Pr = 0.28158), but varied with provided N:P ratio (*F* = 12.477, Pr < 0.001) and showed a significant interaction (F = 3.308, Pr = 0.00147) (Fig.2a). The variation was non-linear and the difference (Δ = Max. – Min.) was greater for samples without Cu (0.24 mmol g^{-1})

compared to the one with 1 µM and 15 µM of Cu (0.11 mmol g^{-1} and 0.13 mmol g^{-1}, respectively). Since the global average of immobilized N was around 0.17 mmol g^{-1}, the percentage of provided N that has been immobilized decreased significantly with increasing N:P ratio (Kruskal-Wallis, $X^2 = 62.998$, $p < 0.001$) (Fig.2b). The quantity of immobilized P was lower at 15 µM [Cu] ($X^2 = 8.5283$, $p = 0.01406$) and decreased with increasing N:P ratio ($X^2 = 38.221$, $p < 0.001$) (Fig.2c). As a result, the percentage of provided P that has been immobilized increased significantly with increasing N:P ratio ($X^2 = 44.306$, $p < 0.001$) and lower with [Cu] ($X^2 = 6.8641$, $p = 0.03232$) (Fig.2d). As a proxy of the microbial N:P ratio, the ratio of immobilized N:P ranged from 12 to 125, with a 10-fold increase with increasing of the provided N:P ratio and up to 3-fold at the higher [Cu]. The condition with 15 µM of Cu showed a greater intra-replicate variation and higher immobilized N:P ratios compared to the 0 and 1 µM of Cu (Fig.2e).

3.3. Identification of the cellulose decomposition actors

The relative abundance of bacteria and fungi was estimated through qPCR quantification of 16S and 18S rRNA genes. The relative proportion of bacteria to fungi (Fig.3) was not changed by N:P ratios ($X^2 = 1.8853$, $p = 0.9299$) but significantly decreased 10 folds with increasing [Cu] ($X^2 = 42.229$, $p < 0.001$). Abundance of bacterial 16S was about 10^3 to 10^5 times higher than that of fungi. The 16S rRNA gene copies stayed relatively constant (10^6 to 10^7 copies μL^{-1}) among the provided N:P ratios ($X^2 = 12.733$, $p = 0.04748$) and [Cu] ($X^2 = 3.943$, $p = 0.1392$). The number of 18S rRNA gene copies was not influenced by N:P ratios ($X^2 = 1.2234$, $p = 0.9757$), but increased with [Cu] from 10^2 to 10^4 copies μL^{-1} ($X^2 = 46.624$, $p < 0.001$) (See Fig.S3). The ergosterol assays also confirm the low abundance of fungi since ergosterol was detected only on 2 out of 21 samples analysed (0.08 and 0.20 µg ml^{-1} compared to at least 4.15 µg ml^{-1} for positive controls, which correspond to 7.1 and 26.4 µg g^{-1} of cellulose disc). All these results indicated that cellulose discs were mainly colonized by

bacterial communities confirming our visual observations made during incubations (no fungal mycelium development on cellulose disc surface).

3.4. Bacterial community diversity

Since bacteria were dominant, only bacterial community diversity was assessed through 16S rDNA sequencing. Alpha-diversity indices are shown in Fig.S4. The Chao1 index indicated that the mean bacterial species richness decreased with increasing N:P ratio (X^2 = 14.126, p = 0.04898) and with increasing [Cu] (X^2 = 48.128, p < 0.001). The Shannon index showed that the bacterial diversity stayed relatively constant for all tested [Cu] (F = 5.079, Pr < 0.001). For bacterial communities exposed to 0 and 1 µM [Cu], the diversity index values were lower for high N:P ratio indicating the emergence of very abundant taxa. Higher variability in Shannon diversity indices was observed with increasing [Cu] (Levene's Test, F = 6.4451, Pr < 0.001) indicating a higher intra-replicate heterogeneity.

Linear correlations between cellulose mass loss and OTU numbers, Chao1 richness or Shannon diversity indices of all three Cu contamination levels are shown in Fig.4. For 0 and 1 µM of Cu, cellulose mass loss was positively correlated with the OTU number, Chao1 index and Shannon index. For 15 µM Cu, similar correlation was found between cellulose mass loss and Chao1 index, but no correlation was found with OTU number and Shannon index. The variation in richness was minimal compared to that of the mass loss.

The bacterial taxonomic diversity for each condition is shown in Fig.5 as the relative abundance of the five major phyla and the major *Proteobacteria* class (i.e. *Gammaproteobacteria*) representing more than 10% of the sequences. The relative abundance of each phylum was significantly different between N:P ratios and between [Cu]. The bacterial communities from conditions with 0 and 1 µM of [Cu] were dominated by either *Gammaproteobacteria* at lower N:P ratio, by *Bacteroidetes* at higher N:P ratio or by *Chloroflexi* regardless of the N:P ratio. In the microcosms with the higher [Cu] (15 µM), the

bacterial community was dominated either by *Bacteroidetes* at lower N:P ratio, or by *Gammaproteobacteria, Firmicutes* and *Actinobacteria* at higher N:P ratio. *Actinobacteria* and *Firmicutes* were stimulated in condition with 15µM of Cu (Wilcoxon-Mann Whitney test, p <0.001 for both phyla). The relative proportion of *Chloroflexi* decreased at the higher [Cu] (p < 2e-16).

Beta diversity of the communities developing in all the tested conditions was shown through NMDS analyses (Fig.6). Samples were clearly separated (first dimension, NMDS1) based on the [Cu] (Fig.6a). A higher variability among samples exposed to 15 µM of Cu was observed compared to 0 and 1µM of Cu. A shift in the community composition was highlighted according to the N:P ratios mainly for samples exposed at higher [Cu] (separation on the second dimension NMDS2; Fig.6b). PerMANOVA analyses confirmed the significant difference of the community composition between each of the three [Cu] ($F = 10.795$, $p = 0.001$), while the difference was lower but also significant between each of the seven N:P ratios ($F = 1.365$, $p = 0.024$).

The results of indicator species analysis with indicator values are shown in Fig.S5. The reasons behind our decision of merging the conditions into four groups are, firstly bacterial diversities with 0 and 1 µM of [Cu] were similar compared to that of 15 µM of [Cu], and secondly cellulose decompositions at N:P ratios lower than 33 at different [Cu] varied compared to that at ratios higher than 33 which stayed constant. For the group CLRL (low copper, low ratios), there were 11 indicators of which four *Bacteroidetes*, three *Gammaproteobacteria* and four *Verrucomicrobia*. For the group CLRH (low copper, high ratios), there were two indicators of which one *Bacteroidetes* and one *Gammaproteobacteria*. For the group CHRL (high copper, low ratios), there were nine indicators of which seven *Bacteroidetes*, one *Gammaproteobacteria* and one *Verrucomicrobia*. For the group CHRH (high copper, high ratios), there were ten indicators of which one *Bacteroidetes*, four

Gammaproteobacteria, one *Firmicutes*, and four *Actinobacteria*. The analysis also revealed 15 indicator species related to the combination of groups CLRL and CLRH, which is equivalent to the group with low copper (CL). And finally, four indicator species for the groups of CHRL and CHRL, which is the equivalent to the group with high copper (CH). For the group CL, there were five *Bacteroidetes*, three *Gammaproteobacteria*, five *Chloroflexi* and one *Verrucomicrobia*. For the group CH, there were three *Bacteroidetes* and one *Gammaproteobacteria*. More detailed information can be found under Fig.S5.

4. Discussion

4.1. General observations

Cellulose decomposition was maximized at an optimal N:P ratio with, or without copper contamination. Copper contamination had no significant effect on the maximal decomposition rate around the optimal N:P ratio but had strongly reduced the range of the ratio in which cellulose decomposition can occur. These changes were followed by large shifts in bacterial community compositions. Bacteria sensitivities toward the contaminant and the relative N:P availability in environment can both select particular taxa within a bacterial decomposer community.

Despite the use of a natural microbial inoculum, fungal spores were not present in our inoculum, and fungi hardly developed in our microcosms. Some possible explanations might be that we have collected the leaf bags at a late stage of decomposition. During inoculum preparation, partially decomposed leaves were reduced into small pieces instead of staying intact as we usually get while inducing fungal spores. This observation is consistent with the common assumption that bacteria only become abundant at a later stage on small leaf litter fragments (Sinsabaugh and Findlay 1995). The decantation step we applied in the inoculum to limit the risk of introducing leaf litter fragments in our microcosms might also have participated in the absence of fungal spores. Finally, aquatic hyphomycetes that were

expected to be present in our inoculum generally require very high levels of oxygen to maintain their activity (Medeiros, Pascoal and Graça 2009) and our microcosms, leading to the development of a few anaerobic taxa (see section 4.2), were certainly not perfectly adapted for ensuring their development. As a result, bacteria were largely dominant under all tested conditions, and we ultimately decided to focus on bacterial communities for taxonomic analysis.

4.2. Stoichiometric demand of microbial decomposers for cellulose decomposition

In our study, cellulose decomposition was largely controlled by ratios of dissolved inorganic N and P in the medium. As predicted by our first hypothesis (H1), the decomposition rate reached its maximum at a dissolved N:P ratio of 4.7. At this particular N:P ratio, N and P availabilities were certainly co-limiting microbial activity allowing an optimal decomposition of the carbon substrate. The occurrence of such a bell-shaped response of cellulose decomposition had already been observed by Güsewell and Gessner (2009), by using a natural microbial inoculum containing both bacteria and fungi. At the same nutrient supply level, they have found an optimal mass N:P ratio for cellulose decomposition of 15 (33 molar ratio), which is higher than the optimal N:P ratio found in our study. Meanwhile, the same authors also found that bacterial development was maximized at lower environmental N:P ratios than for fungal development. In our study, microbial communities were largely dominated by bacteria, and the low optimal N:P ratio we observed might be explained by this dominance. Bacteria and fungi have different nutrient requirements, yet both are found to be flexible. This flexibility is the result of differences in cellular contents and processes between bacteria and fungi (Godwin and Cotner 2018; Camenzind *et al.* 2020a, 2020b). The differences in nutrient requirements between bacteria and fungi can directly affect their competitive abilities and dominance on different substrates (Danger, Gessner and Bärlocher 2016).

In the absence of Cu contaminant, significant cellulose mass losses were observed throughout the whole N:P ratio range tested, even when the medium was extremely depleted in P (high N:P ratio). Mass loss was always above 8 %. This result suggests that even though the decomposition rate was reduced outside the optimal N:P ratio of the given microbial decomposer community, this process was never fully stopped. Nevertheless, it was not possible to follow decomposition kinetics using a single sampling date. The next step will be to verify if stoichiometric imbalances would mostly slow down the decomposition process or if this process would eventually stop due to nutrient unavailability.

Although the average quantity of N immobilized on cellulose disc stayed at a relatively constant level around 0.17 mmol g^{-1} of dry cellulose disc, N immobilization was not linear along the gradient of N:P ratios tested. The quantity of N immobilized was maximized at the optimal N:P ratio for cellulose decomposition and minimized at the N:P ratio where the minimal decomposition rate occurred. The portion of N immobilized increased when the ratio was low. This result agrees with that of Güsewell and Gessner (2009), showing that decomposers were more efficient at immobilizing N when it was the most limiting element. The quantity of P immobilized followed a similar profile as cellulose decomposition rate, i.e. a bell-shaped response, P immobilization was maximized at an N:P ratio of 3.7. The proportion of total P immobilized increased when N:P ratios were high, suggesting the decomposers immobilize P more efficiently when it is the limiting element. This observation, however, contrasts with the previous observations of Güsewell and Gessner (2009). A possible explanation could be related to the very low abundance of fungi in our study, since fungi are known to be able to store large amounts of extra P as polyphosphates when P is not limiting (Beever and Burns 1981).

Interestingly, bacterial species richness dropped significantly for the highest N:P ratio, where cellulose decomposition rate slowed down to its minimum. As already observed in

previous studies (e.g. Leflaive *et al.* 2008; Lemmel *et al.* 2019), our results evidenced positive correlations between the intensity of microbial functions and the diversity: cellulose mass losses were significantly and positively related to bacteria OTU numbers, Chao1 richness and Shannon diversity indices. This suggests that only a few bacterial taxa are capable of surviving in environment with highly imbalanced N and P, and these species are probably less efficient in decomposing cellulose under high N:P ratios. When looking more specifically to the taxa present along the N:P gradient, we found that the relative abundance of *Gammaproteobacteria* was strongly related to cellulose decomposition efficiency, these being more abundant around the optimal N:P ratio. Bacteria from this class probably carried out most of the decomposition in our study. Even if we cannot exclude the possibilities that certain bacteria with low abundances can also be very actively involved in decomposition. Although *Gammaproteobacteria* are still present at higher N:P ratios, their abundance decreased in favour of *Chloroflexi* and *Bacteroidetes* which became dominant. Among *Chloroflexi, Anaerolineae* was the dominant class. Although the ecological role of the *Anaerolineae* members remains unclear, these bacteria have been shown to exhibit cellulolytic activities (Hug *et al.* 2013; Xia *et al.* 2016). The detection of these strict anaerobic bacteria suggests that despite the absence of total water immersion, parts of the cellulose discs could have ended up in anaerobic conditions. For the highest N:P ratio, *Bacteroidetes* represented up to 75 % of total abundance. *Verrucomicrobia* was shown to be less abundant yet consistently present throughout all the N:P ratios. A recent study has argued a possible under estimation of its abundance due to methodological biases (Chiang *et al.* 2018). All these findings confirm partially our fourth hypothesis (H4) that N:P ratio strongly contributes to the composition of active bacterial communities. Even though the functional redundancy among bacterial decomposers could ensure basal cellulose decomposition, the activities of these different active taxa at different N:P ratios were not equally efficient.

4.3. Stoichiometric demand for cellulose decomposition in the presence of copper

In the presence of Cu in the microcosms, the overall cellulose decomposition remained unchanged in the presence of copper when N:P ratios were close to microbial stoichiometric optimal requirements, whatever the copper concentration tested. For the highest Cu concentration (15 µM of Cu), cellulose mass loss was significantly reduced when deviating from this optimal ratio. This observation partly confirms our second hypothesis that high Cu concentration would reduce cellulose decomposition rates (H2) and is consistent with previous studies investigating copper effects on leaf litter decomposition (Roussel, Chauvet and Bonzom 2008; Ferreira *et al.* 2016) and alter the structure of bacterial decomposer community (Duarte *et al.* 2008). This result might be due to direct Cu toxicity which has long been evidenced for both bacteria and fungi (e.g. Dupont, Grass and Rensing 2011).

Contrary to our expectation (see hypothesis H3), the optimal N:P ratio for maximal cellulose decomposition rate decreased with raising Cu concentration. Cu at low concentrations is known to be an essential microelement (Cervantes and Gutierrez-Corona 1994), metal-transporting-proteins which regulate multiple metal homoeostasis (including Cu) are naturally present on bacterial membranes to regulate intracellular metal concentrations. Cu(II) ion appears to be less toxic than Cu(I), as we introduced Cu(II) from $CuSO_4$, bacteria were exempt from synthesizing Cu(I)-detoxification-proteins (Ladomersky and Petris 2015), which would have required more N. Cu(II) export, on the other hand, does not require synthesizing additional transporters, but mainly relies on existing ATP-dependent proteins to actively relocate Cu outside the cell membrane (Ma, Jacobsen and Giedroc 2009). A stronger increase in energetic requirements (and thus in P-rich molecules, such as ATP) than in the production of N-rich detoxification proteins might be a plausible explanation of why the optimal N:P ratio for decomposition had decreased.

Our results also highlighted that the minimal cellulose mass losses under high Cu contamination (close to 0 %) were significantly lower than those of control and low Cu contamination treatment (which always remained above 8%, whatever the N:P ratio tested). In other words, rather than keeping a slow but non-zero rate of decomposition, high Cu contamination arising concomitantly with N:P ratios higher than 33 had led to a total stop of cellulose decomposition. As pointed out by Peñuelas *et al.* (2013), anthropic input of N into the biosphere is excessively higher than that of P, creating an increasingly imbalanced environmental N:P ratio, This N:P imbalance alone had already affected the life histories of microorganisms and other life forms (Elser *et al.* 2009). In case of high Cu contamination, it could take the decomposition process to halt and effectively stop carbon turnover. Our findings suggest that human-induced global nutrient imbalances might lead to exacerbated responses of microbial processes in presence of contaminants.

Copper reduced the richness of the bacteria community at each N:P ratio even at the lowest level test. For the highest copper concentration, the effect of N:P ratios over bacterial richness was minimized, suggesting a higher selective pressure of Cu rather than N:P balances on bacterial communities. Cellulose decomposition blocked in both high N:P and high copper conditions could be partly explained by the elimination, or at least a decrease in abundance of certain cellulolytic taxa that are sensitive to high Cu concentrations, and their replacement (with similar abundance) by Cu-tolerant taxa (Indicator species: *Flavobacterium*, *Nitrosospira*, *Pseudomonas*, *Aeromonas*, *Variovorax*, *Paenibacillus* and *Nocardiaceae*) probably less efficient or even incapable of decomposing cellulose. The positive correlations between cellulose mass losses and OTU numbers, richness and diversity of the bacterial community observed in control and low Cu conditions almost disappeared in the presence of 15µM of copper. This means that in the most contaminated conditions, the community richness had little to do with cellulose mass loss, which suggests a shift in the community

composition and taxa replacements. As shown that *Bacteroidetes* dominance were replaced by *Gammaproteobacteria, Firmicutes* and *Actinobacteria* from low to high N:P ratio. Different indicator species were also identified under different situations. All these observations confirm our hypothesis (H4) that the contaminant and the N:P ratio in the environment interactively control microbial community structure, with large consequences on their functions and activities (i.e. cellulose decomposition).

5. Conclusion

Bacteria were the main decomposers in our study. Without copper contamination, cellulose decomposition was maximized at an N:P molar ratio of 4.7. Both N and P immobilization by bacterial decomposers were more efficient when these elements were the limiting ones. Bacterial species diversity and richness dropped at high N:P ratios (when P was limited) but the community as a whole maintained a basal level of cellulose decomposition.

Overall, the lowest Cu concentration tested had little to no negative effect over bacterial decomposer communities, their taxonomic compositions, their N and P stoichiometric demands, and their capacity to decompose cellulose. In contrast, at the highest Cu concentration tested, the composition of bacterial communities was drastically reshaped, which had significantly reduced the optimal N:P ratio for cellulose decomposition to 2.8, and negatively affected the global cellulose decomposition efficiency in the most stoichiometrically imbalanced conditions (the highest N:P ratios). In this study, we focused on cellulose decomposition, but other microbial functions could be simultaneously affected and would require further studies. For example, Cu has been shown to inhibit bacterial glucose utilization, or nitrifiers and denitrifiers metabolic activities (Ochoa-Herrera *et al.* 2011). To conclude, the current increased imbalance between N and P availabilities on Earth, which correspond to a major parameter of global change, might lead to unexpected interactions with other stressors, in turn largely impacting microbial functions. Our results shed the light on a

potentially important and understudied environmental problem that could have large repercussions on ecosystem functioning worldwide.

Funding

This work was supported by the French National Research Agency through ANR project "StoichioMic" (ANR 18 CE32 0003 01).

Acknowledgement

We are grateful to Mr Q. Bachelet for fields and technical support, to Mr P. Rousselle for conducting chemical analyses, and to three anonymous reviewers for their constructive comments on an earlier draft of this manuscript.

Conflict of Interest

The authors declare no conflict of interest.

References

Bani A, Pioli S, Ventura M *et al.* The role of microbial community in the decomposition of leaf litter and deadwood. *Applied Soil Ecology* 2018;**126**:75–84.

Beever RE, Burns DJW. Phosphorus Uptake, Storage and Utilization by Fungi. *Advances in Botanical Research* 1981;**8**:127–219.

Berg B, Ekbohm G, Söderström B *et al.* Reduction of decomposition rates of scots pine needle litter due to heavy-metal pollution. *Water, Air, and Soil Pollution* 1991;**59**:165–77.

Camenzind T, Lehmann A, Ahland J *et al.* Trait-based approaches reveal fungal adaptations to nutrient-limiting conditions. *Environmental Microbiology* 2020;**22**:3548–60.

Camenzind T, Grenz K, Lehmann J *et al.* Soil fungal mycelia have unexpectedly flexible stoichiometric C:N and C:P ratios. *Ecology Letters* 2021;**24**:208–218.

Caporaso JG, Lauber CL, Walters WA *et al.* Global patterns of 16S rRNA diversity at a depth of millions of sequences per sample. *Proc Natl Acad Sci U S A* 2011;**108**:4516–22.

Cébron A, Norini MP, Beguiristain T *et al.* Real-Time PCR quantification of PAH-ring hydroxylating dioxygenase (PAH-RHDα) genes from Gram positive and Gram negative bacteria in soil and sediment samples. *Journal of Microbiological Methods* 2008;**73**:148–59.

Cervantes C, Gutierrez-Corona F. Copper resistance mechanisms in bacteria and fungi. *FEMS Microbiology Reviews* 1994;**14**:121–37.

Chew I, Obbard JP, Stanforth RR. Microbial cellulose decomposition in soils from a rifle range contaminated with heavy metals. *Environmental Pollution* 2001;**111**:367–75.

Chiang E, Schmidt ML, Berry MA *et al.* Verrucomicrobia are prevalent in north-temperate freshwater lakes and display class-level preferences between lake habitats. *PLoS ONE* 2018;**13**:1–20.

Cornwell WK, Cornelissen JHC, Amatangelo K *et al.* Plant species traits are the predominant control on litter decomposition rates within biomes worldwide. *Ecology Letters* 2008;**11**:1065–71.

Danger M, Daufresne T, Lucas F *et al.* Does Liebig's law of the minimum scale up from species to communities? *Oikos* 2008;**117**:1741–51.

Danger M, Gessner MO, Bärlocher F. Ecological stoichiometry of aquatic fungi: Current knowledge and perspectives. *Fungal Ecology* 2016;**19**:100–11.

Daufresne T, Loreau M. Ecological stoichiometry, primary producer-decomposer interactions, and ecosystem persistence. *Ecology* 2001;**82**:3069–82.

de Cáceres M, Legendre P, Moretti M. Improving indicator species analysis by combining groups of sites. *Oikos* 2010;**119**:1674–84.

Demircan T, Ovezmyradov G, Yıldırım B *et al.* Experimentally induced metamorphosis in highly regenerative axolotl (ambystoma mexicanum) under constant diet restructures microbiota. *Scientific Reports* 2018;**8**:1–13.

Duarte S, Pascoal C, Alves A *et al.* Copper and zinc mixtures induce shifts in microbial communities and reduce leaf litter decomposition in streams. *Freshwater Biology* 2008;**53**:91–101.

Dupont CL, Grass G, Rensing C. Copper toxicity and the origin of bacterial resistance - New insights and applications. *Metallomics* 2011;**3**:1109–18.

Elser JJ, Andersen T, Baron JS *et al.* Shifts in lake N: P stoichiometry and nutrient limitation driven by atmospheric nitrogen deposition. *Science (1979)* 2009;**326**:835–7.

Falkowski P, Scholes RJ, Boyle E *et al.* The global carbon cycle: A test of our knowledge of earth as a system. *Science (1979)* 2000;**290**:291–6.

Fanin N, Fromin N, Buatois B *et al.* An experimental test of the hypothesis of non-homeostatic consumer stoichiometry in a plant litter-microbe system. *Ecology Letters* 2013;**16**:764–72.

Fernández D, Voss K, Bundschuh M *et al.* Effects of fungicides on decomposer communities and litter decomposition in vineyard streams. *Science of the Total Environment* 2015;**533**:40–8.

Ferreira R, Gaspar H, Gonzalez JM *et al.* Copper and temperature modify microbial communities, ammonium and sulfate release in soil. *Journal of Plant Nutrition and Soil Science* 2015a;**178**:953–62.

Ferreira V, Castagneyrol B, Koricheva J *et al.* A meta-analysis of the effects of nutrient enrichment on litter decomposition in streams. *Biological Reviews* 2015b;**90**:669–88.

Ferreira V, Koricheva J, Duarte S *et al.* Effects of anthropogenic heavy metal contamination on litter decomposition in streams - A meta-analysis. *Environmental Pollution* 2016;**210**:261–70.

Fox J, Weisberg S. *An {R} Companion to Applied Regression*. Third. Thousand Oaks {CA}: Sage, 2019.

Frost PC, Benstead JP, Cross WF *et al.* Threshold elemental ratios of carbon and phosphorus in aquatic consumers. *Ecology Letters* 2006;**9**:774–9.

Ge X, Zeng L, Xiao W *et al.* Effect of litter substrate quality and soil nutrients on forest litter decomposition: A review. *Acta Ecologica Sinica* 2013;**33**:102–8.

Gessner MO, Chauvet E, Dobson M. A Perspective on Leaf Litter Breakdown in Streams. *Oikos* 1999;**85**:377.

Gessner MO, Swan CM, Dang CK *et al.* Diversity meets decomposition. *Trends in Ecology and Evolution* 2010;**25**:372–80.

Gessner MO. Ergosterol as a Measure of Fungal Biomass. *Methods to Study Litter Decomposition*. Vol 69. Berlin/Heidelberg: Springer-Verlag, 2005, 189–95.

Godwin CM, Cotner JB. What intrinsic and extrinsic factors explain the stoichiometric diversity of aquatic heterotrophic bacteria? *ISME Journal* 2018;**12**:598–609.

Güsewell S, Gessner MO. N:P ratios influence litter decomposition and colonization by fungi and bacteria in microcosms. *Functional Ecology* 2009;**23**:211–9.

Güsewell S, Verhoeven JTA. Litter N:P ratios indicate whether N or P limits the decomposability of graminoid leaf litter. *Plant and Soil* 2006;**287**:131–43.

Harte J, Kinzig AP. Mutualism and competition between plants and decomposers: implications for nutrient allocation in ecosystems. *American Naturalist* 1993;**141**:829–46.

Hill TCJ, Walsh KA, Harris JA *et al.* Using ecological diversity measures with bacterial communities. *FEMS Microbiology Ecology* 2003;**43**:1–11.

Hopkins DW, Ibrahim DM, O'donnell AG *et al.* Decomposition of cellulose, soil organic matter and plant litter in a temperate grassland soil. *Plant and Soil* 1990;**124**:79–85.

Hug LA, Castelle CJ, Wrighton KC *et al.* Community genomic analyses constrain the distribution of metabolic traits across the Chloroflexi phylum and indicate roles in sediment carbon cycling. *Microbiome* 2013;**1**:1–17.

Keiblinger KM, Schneider M, Gorfer M *et al.* Assessment of Cu applications in two contrasting soils—effects on soil microbial activity and the fungal community structure. *Ecotoxicology* 2018;**27**:217–33.

Kilham SS, Kreeger DA, Lynn SG *et al.* COMBO: a defined freshwater culture medium for algae and zooplankton. *Hydrobiologia* 1998;**377**:147–59.

Kozich JJ, Westcott SL, Baxter NT *et al.* Development of a dual-index sequencing strategy and curation pipeline for analyzing amplicon sequence data on the miseq illumina sequencing platform. *Applied and Environmental Microbiology* 2013;**79**:5112–20.

Ladomersky E, Petris MJ. Copper tolerance and virulence in bacteria. *Metallomics* 2015;**7**:957–64.

Larras F, Billoir E, Baillard V *et al.* DRomics: A Turnkey Tool to Support the Use of the Dose-Response Framework for Omics Data in Ecological Risk Assessment. *Environmental Science and Technology* 2018;**52**:14461–8.

Leflaive J, Danger M, Lacroix G *et al.* Nutrient effects on the genetic and functional diversity of aquatic bacterial communities. *FEMS Microbiology Ecology* 2008;**66**:379–90.

Lemmel F, Maunoury-Danger F, Leyval C *et al.* DNA stable isotope probing reveals contrasted activity and phenanthrene-degrading bacteria identity in a gradient of anthropized soils. *FEMS Microbiology Ecology* 2019;**95**:1–14.

Ma Z, Jacobsen FE, Giedroc DP. Coordination chemistry of bacterial metal transport and sensing. *Chemical Reviews* 2009;**109**:4644–81.

Medeiros AO, Pascoal C, Graça MAS. Diversity and activity of aquatic fungi under low oxygen conditions. *Freshwater Biology* 2009;**54**:142–9.

Moore JC, Berlow EL, Coleman DC *et al.* Detritus, trophic dynamics and biodiversity. *Ecol Lett* 2004;**7**:584–600.

Muyzer G, de Waal EC, Uitterlinden AG. Profiling of complex microbial populations by denaturing gradient gel electrophoresis analysis of polymerase chain reaction-amplified genes coding for 16S rRNA. *Applied and Environmental Microbiology* 1993;**59**:695–700.

Niyogi DK, Cheatham CA, Thomson WH *et al.* Litter breakdown and fungal diversity in a stream affected by mine drainage. *Fundamental and Applied Limnology* 2009;**175**:39–48.

Nübel U, Engelen B, Felsre A *et al.* Sequence heterogeneities of genes encoding 16S rRNAs in Paenibacillus polymyxa detected by temperature gradient gel electrophoresis. *Journal of Bacteriology* 1996;**178**:5636–43.

Ochoa-Herrera V, León G, Banihani Q *et al.* Toxicity of copper(II) ions to microorganisms in biological wastewater treatment systems. *Science of the Total Environment* 2011;**412–413**:380–5.

Oksanen J, Blanchet FG, Friendly M *et al.* Package "vegan" Title Community Ecology Package Version 2.5-7. *cran.ism.ac.jp* 2020.

Peñuelas J, Poulter B, Sardans J *et al.* Human-induced nitrogen-phosphorus imbalances alter natural and managed ecosystems across the globe. *Nature Communications* 2013;**4**, DOI: 10.1038/ncomms3934.

R Core Team. R: A Language and Environment for Statistical Computing. 2022.

Roussel H, Chauvet E, Bonzom JM. Alteration of leaf decomposition in copper-contaminated freshwater mesocosms. *Environmental Toxicology and Chemistry* 2008;**27**:637–44.

Schloss PD, Westcott SL, Ryabin T *et al.* Introducing mothur: Open-source, platform-independent, community-supported software for describing and comparing microbial communities. *Applied and Environmental Microbiology* 2009;**75**:7537–41.

Sinsabaugh RL, Findlay S. Microbial production, enzyme activity, and carbon turnover in surface sediments of the Hudson River estuary. *Microbial Ecology: An International Journal* 1995;**30**:127–41.

Smit E, Leeflang P, Glandorf B *et al.* Analysis of fungal diversity in the wheat rhizosphere by sequencing of cloned PCR-amplified genes encoding 18S rRNA and temperature

gradient gel electrophoresis. *Applied and Environmental Microbiology* 1999;**65**:2614–21.

Solé M, Fetzer I, Wennrich R *et al.* Aquatic hyphomycete communities as potential bioindicators for assessing anthropogenic stress. *Science of the Total Environment* 2008;**389**:557–65.

Sterner RW, Elser JJ. Ecological Stoichiometry: The Biology of Elements from Molecules to the Biosphere. *Ecological Stoichiometry: The Biology of Elements from Molecules to the Biosphere*. Princeton University Press, 2002, 439.

Tessier JT, Raynal DJ. Use of nitrogen to phosphorus ratios in plant tissue as an indicator of nutrient limitation and nitrogen saturation. *Journal of Applied Ecology* 2003;**40**:523–34.

Thion C, Cébron A, Beguiristain T *et al.* Long-term in situ dynamics of the fungal communities in a multi-contaminated soil are mainly driven by plants. *FEMS Microbiology Ecology* 2012;**82**:169–81.

Tilman D. The Resource-Ratio Hypothesis of Plant Succession. *The American Naturalist* 1985;**125**:827–52.

Tolkkinen M, Mykrä H, Annala M *et al.* Multi-Stressor impacts on fungal diversity and ecosystem functions in streams: natural vs. anthropogenic stress. *Ecology* 2015;**96**:672–83.

Vainio EJ, Hantula J. Direct analysis of wood-inhabiting fungi using denaturing gradient gel electrophoresis of amplified ribosomal DNA. *Mycological Research* 2000;**104**:927–36.

Wakelin SA, Chu G, Lardner R *et al.* A single application of Cu to field soil has long-term effects on bacterial community structure, diversity, and soil processes. *Pedobiologia (Jena)* 2010;**53**:149–58.

Woodward G, Gessner MO, Giller PS *et al.* Continental-scale effects of nutrient pollution on stream ecosystem functioning. *Science (1979)* 2012;**336**:1438–40.

Xia Y, Wang Y, Wang Y *et al.* Cellular adhesiveness and cellulolytic capacity in Anaerolineae revealed by omics-based genome interpretation. *Biotechnology for Biofuels* 2016;**9**:1–13.

Zhang T, Luo Y, Chen HYH *et al.* Responses of litter decomposition and nutrient release to N addition: A meta-analysis of terrestrial ecosystems. *Applied Soil Ecology* 2018;**128**:35–42.

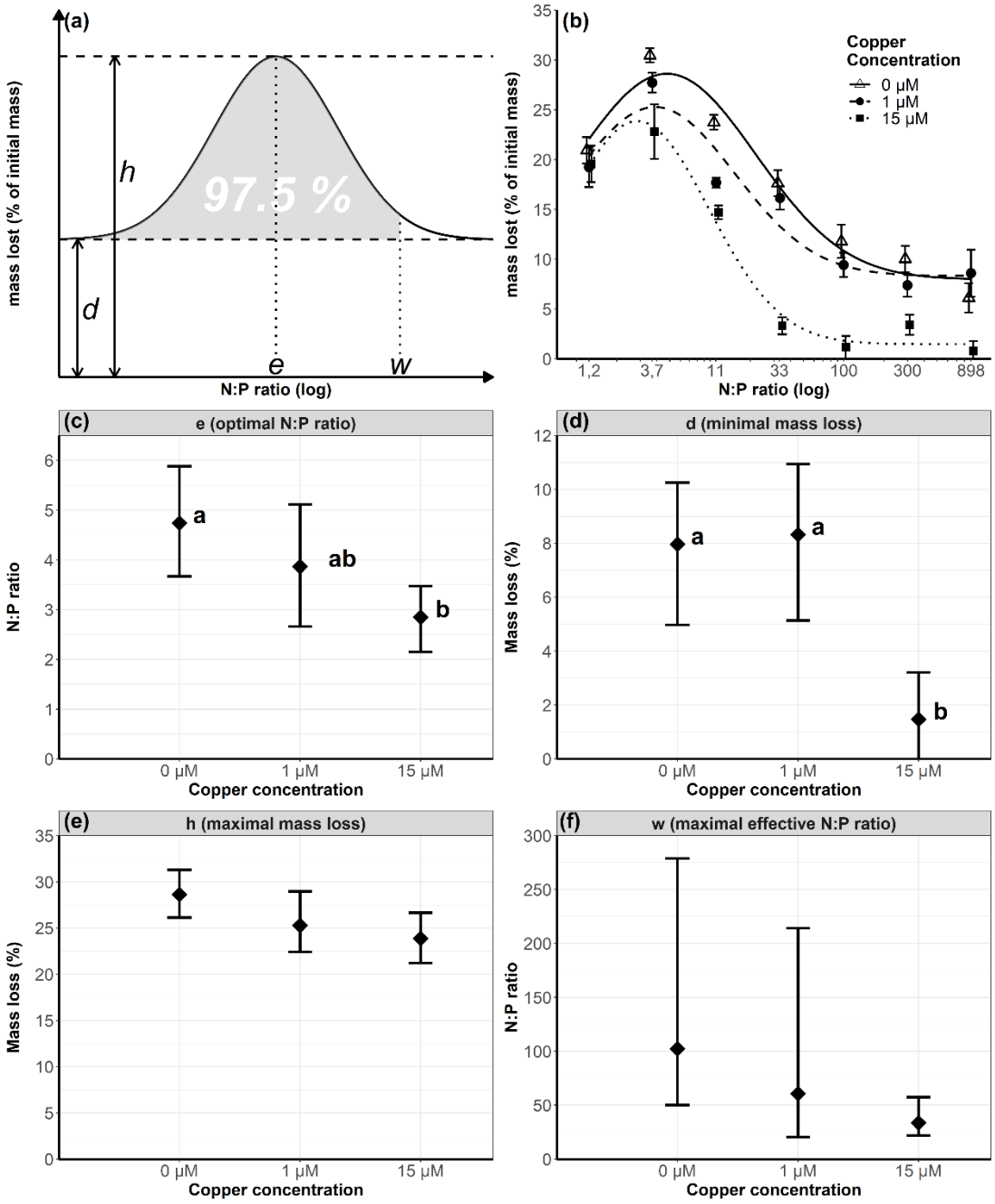

Figure 1 – (a) Schematic representation of the Gaussian model. *x-axis* is the log transformed N:P ratios; *y-axis* is the mass loss. ***d*** is the minimal mass loss; ***h*** is the maximal mass loss; ***e*** is the optimal N:P ratio for the maximal mass loss; ***w*** is the maximal effective N:P ratio less than which there are 97.5 % of cumulative mass loss from the level of ***d*** (grey area). **(b) Cellulose mass losses**. Cellulose disc mass losses after 79 days, calculated in percentage of the average initial mass (36.3 mg) minus the average 3% loss of the controls without inoculum. *x-axis* for provided N:P ratios is log-transformed but shows as the molar ratio for reading convenience. Curves show mass loss calculated by the Gaussian model. **(c, d, e, f) Graphical representation of each parameter estimated by the gaussian model for all three tested copper concentration levels.** The error bars show the 95 % confidence interval (CI) for each estimation.

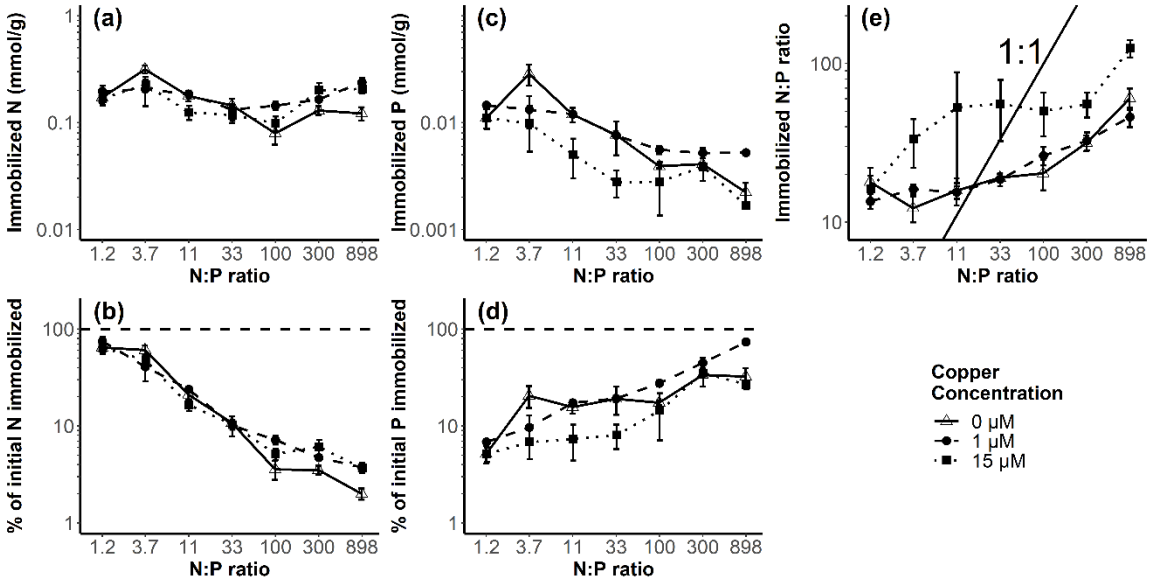

Figure 2 – N and P immobilized on cellulose disc for three copper concentrations in relation to the provided N:P ratio. (a, c) millimoles of N and P immobilized per gram of final cellulose dry mass; **(b, d)** percentage of provided N and P immobilized on the disc; **(e)** immobilized N:P ratio, the 1:1 line shows the immobilized N and P in proportion to the provided ratio. Error bars show the standard deviation of 4 replicates for 0 copper, and 3 replicates for 1 µM and 15 µM copper. x-axis for provided N:P ratios is log-transformed but shows as the molar ratio for reading convenience.

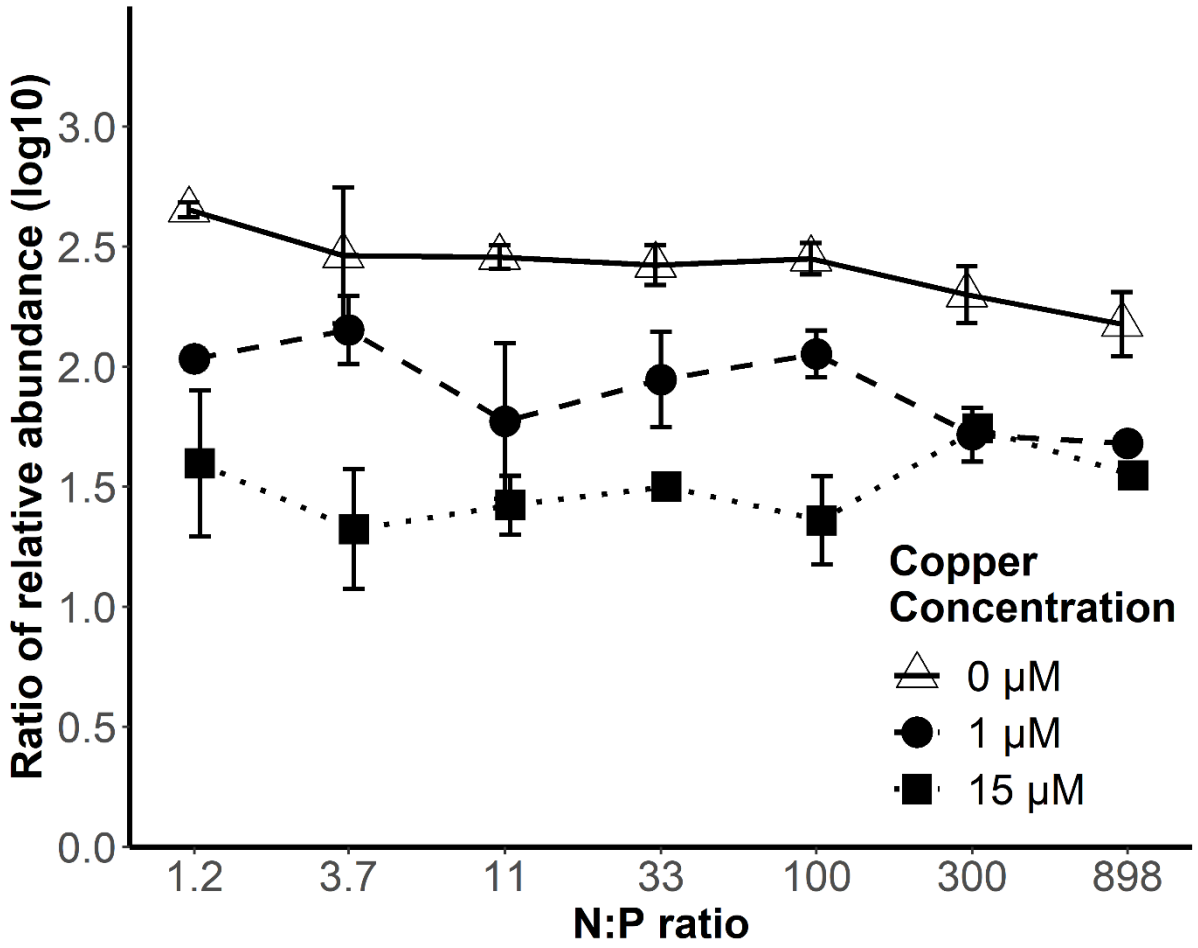

Figure 3 – Ratio between bacterial 16S and fungal 18S rRNA gene copies. *x-axis* for provided N:P ratios is log-transformed but shows as the molar ratio for reading convenience. For the abundances of 16S and 18S rRNA, see Fig.S3.

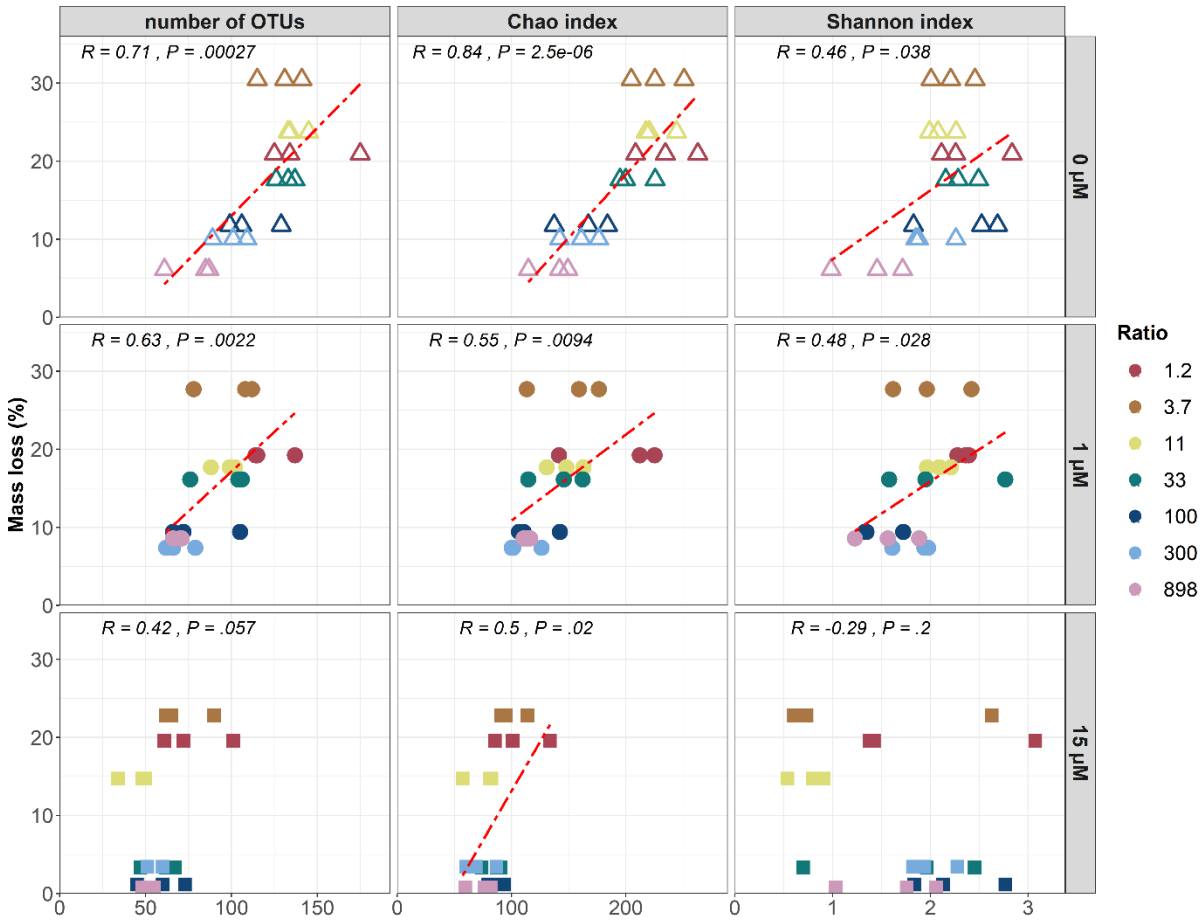

Figure 4 – Linear correlation between mass losses and numbers of OTUs, Chao or Shannon indexes of three Cu contamination levels.

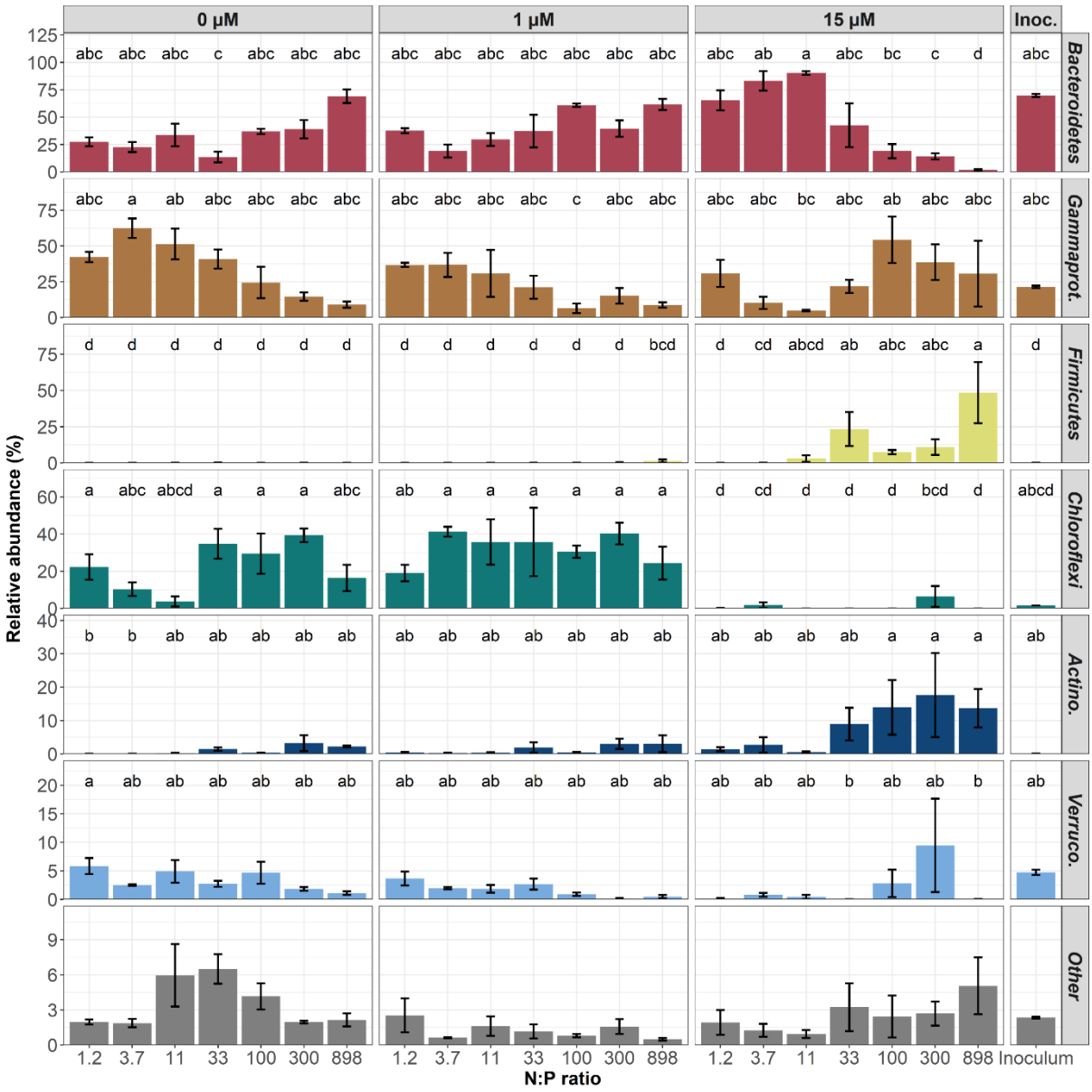

Figure 5 – Bacterial diversity for all three levels of copper contamination and the inoculum. *Gammaprot.*: *Gammaproteobacteria* (class). The rest are shown at phylum level. *Actino.*: *Actinobacteria*, *Verruco.*: *Verrucomicrobia*. Values are the mean abundance of replicates (n =3, for inoculum n = 2). Error bars show the standard deviation between replicates. Letters show significance groups, there is no significant differences between relative abundances in "Other". "Other" groups all OTUs with a relative abundance less than 10 % in any of the replicates. The phyla in the "Other" group are: *Armatimonadetes*, BRC1, *Clamydiae*, *Cyanobacteria*, *Deinococcus-Thermus*, *Dependentiae*, FBP, *Fibrobacteres*, *Hydrogenedentes*, *Lentisphaerae*, *Nitrospirae*, *Planctomycetes*, *Spirochaetes*, unclassified bacteria and *Proteobacteria* (none Gammaproteobacteria).

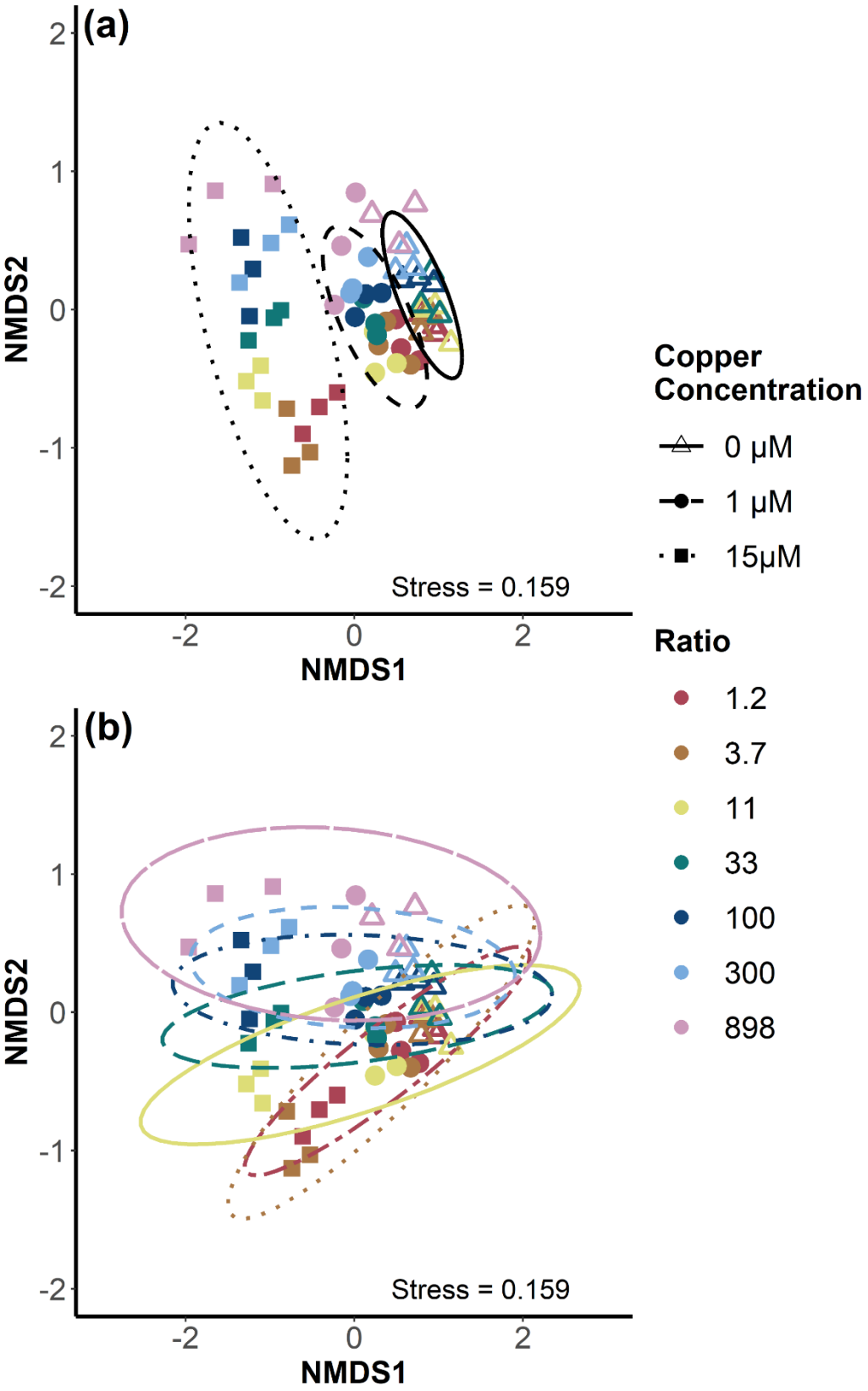

Figure 6 – OTU based beta diversity in NMDS using Bray-Curtis dissimilarity index. **(a)** beta diversity for all tested [Cu]; **(b)** beta diversity for all tested N:P ratios. Ellipses show the 95 % confidence interval.